Molecular structure of extended defects in monolayer-scale pentacene thin films

S. Seo and P. G. Evans[a]
Materials Science Program and Department of Materials Science and Engineering, University of Wisconsin, 1509 University Avenue, Madison, Wisconsin 53706, USA

(Received 11 September 2009; accepted 20 October 2009; published online 25 November 2009)

The growth of pentacene thin films for applications in thin-film transistors and other organic electronic devices results in a variety of extended structural defects including dislocations, grain boundaries, and stacking faults. We have used scanning tunneling microscopy (STM) to probe the molecular-scale structure of grain boundaries and stacking faults in a pentacene thin film on a Si (001) surface modified with styrene. Styrene/Si (001) substrates produce pentacene films that are structurally similar to those grown on insulating substrates, but which are sufficiently smooth and conductive for STM studies. STM images show two types of grain boundaries: in-plane high-angle tilt grain boundaries at the junctions between pentacene islands, and twist boundaries between molecular layers. Segments of the tilt grain boundaries are faceted along low-energy crystallographic directions. Stacking faults are found in the plane of individual pentacene grains. Two rows of molecules near the stacking fault are shifted along the surface normal by 60 pm. Electronically relevant trap states may thus be associated with stacking faults in pentacene thin films. © *2009 American Institute of Physics*. [doi:10.1063/1.3262618]

I. INTRODUCTION

The development of organic electronic materials for applications in electronics, optoelectronics, and photovoltaics fundamentally involves the design and creation of thin films of organic semiconductors.[1] Semiconductors for these applications are polycrystalline thin films, in which the structure and concentration of defece an important role in determining the electrical properties of the resulting materials.[2] In field effect transistors, the difference between the hole mobility of up to 20 $cm^2 V^{-1} s^{-1}$ in devices based on single crystals and thin-film devices with a mobility on the order 1 $cm^2 V^{-1} s^{-1}$ arises in part from structural defects inherent in thin-film growth.[3,4] Charge transfer between the grains of polycrystalline films is disrupted at the highest grain boundary misorientation angles.[5] The mobilities of holes in thin-film transistors based on single grains, however, remain far lower than single-crystal devices, for example, as in Ref. 4. It is thus reasonable to suspect that grain boundaries may not account completely for the lower mobility observed in thin films. In addition, despite the significantly higher hole mobility observed in single-crystal organic electronic devices, it is clear that organic semiconductor single crystals include a large number of structural defects.[6] Other defect structures, in addition to disorder in the interface with the gate insulator and poor charge injection, are likely to be important sources of scattering.

The importance of the structure of extended defects has led to extensive structural characterization of thin films of the molecular organic semiconductor pentacene.[7–9] Extended defects can be probed using both microscopy and diffraction techniques. Diffuse x-ray scattering measurements combined with atomic force microscopy (AFM) have found a significant population of screw dislocations in pentacene thin films.[10] Planar defects, including grain boundaries, have been observed in electron microscopy studies of freestanding nanocrystals.[11,12] Less is known about the molecular structure of defects in pentacene monolayers. In thin-film transistors, a region of the thin film with a thickness first few molecular is particularly important because this is the region in which the carriers arise from a gate electric field.[13] The mobilities of carriers in this region is comparable to thicker films but does not approach the very high values observed in single crystals.[14]

We have used scanning tunneling microscopy (STM) to probe the molecular-scale structure of three distinct types of extended defects in pentacene films with thicknesses of five molecular layers or less. STM provides sufficient spatial resolution to identify individual defects, to determine the orientation of grains, and to search for structural relaxation near defects. Tilt grain boundaries between islands form sharp and crystalline interfaces between islands and consist of a series of short segments of well-defined facets. Twist grain boundaries between the layers of molecules result from the overgrowth of small lower-level islands by larger subsequent islands or from the random nucleation of rotational variants in higher layers. Stacking faults appear within individual grains and exhibit a structural distortion in the rows of molecules immediately adjacent to the interface.

II. EXPERIMENT

The most appropriate substrates for STM studies are flat, chemically and structurally uniform, and exhibit high electrical conductivity. This poses a challenge in characterizing the phases of pentacene relevant to field effect transistor (FET) devices because gate insulators, e.g., SiO_2, are both rough and poor conductors in comparison with the surfaces of met-

[a]Electronic mail: evans@engr.wisc.edu.

 © 2009 American Institute of Physics

Author complimentary copy. Redistribution subject to AIP license or copyright, see http://jap.aip.org/jap/copyright.jsp

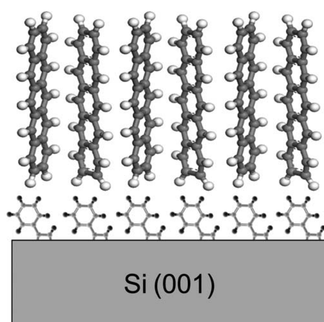

FIG. 1. Schematic structure of a pentacene thin film formed on a styrene-modified Si (001) surface.

als and inorganic semiconductors. Using metal substrates for structural studies of the semiconducting phase of pentacene is problematic because the strong interaction of pentacene with metal surfaces leads to a structure in which the long axes of the pentacene molecules are parallel to the surface, rather than nearly perpendicular as on SiO_2.[7,15] The initial deposition of pentacene on clean Si (001) results in a strongly reacted layer that is structurally quite different from the semiconducting phase of pentacene relevant to thin-film transistors.[16] This problem can be avoided by functionalizing Si (001) with a single layer of small organic molecules to produce modified Si surfaces that are sufficiently conductive and smooth for high-resolution studies.

A schematic of the pentacene thin films on Si (001) surface passivated by a layer of styrene molecule is shown in Fig. 1. Previous studies have shown that a similar structure using cyclopentene rather than styrene results in layers of nearly upright pentacene molecules.[17] Metals can be similarly passivated to allow the appropriate pentacene structure to be formed.[18] The role of the single-molecule-thick layer of styrene in Fig. 1 is simply to prepare a nonreactive surface that allows pentacene layers with a crystallographic structure similar to the structure found in FETs to be grown on a conducting substrate.

The substrate preparation, pentacene deposition, and subsequent STM characterization were performed in ultrahigh vacuum (UHV). The modified Si surface is created by exposing a clean Si (001) surface to a background pressure of styrene molecules. Styrene ($C_6H_5CH{=}CH_2$) forms covalent bonds with Si (001) in which the C atoms of the molecular C–C double bond bridge Si dimers.[19,20] An *ab initio* study predicts that this structure also applies at high coverage and that styrene adsorbs on Si (001) at coverage corresponding to one styrene molecule for occupying each Si dimer.[21]

Styrene-terminated Si (001) surfaces were created starting with *n*-type Si (001) samples ($0.07-0.1\ \Omega$ cm, phosphorus doped) that were cleaned using 3 cycles of the Interuniversity Microelectronics Center (IMEC) process.[22] In each cycle, samples were cleaned in a mixture of H_2SO_4 and H_2O_2 ($H_2SO_4:H_2O_2=4:1$) at 90 °C for 2 min and dipped in 1% HF solution for 2 min to remove the oxide. Finally, a $H_2SO_4-H_2O_2$ solution as used to produce a thin layer of SiO_2. Samples were then loaded into UHV and degassed overnight at ~600 °C. Surfaces exhibiting the (2×1) reconstruction were prepared by heating to 1250 °C for 5 s, cooling rapidly to 1000 °C, and then cooling slowly to room temperature at a rate of 1 °C s^{-1}. The styrene layer was created by exposing the Si surface to styrene at a pressure of 1.0×10^{-7} Torr for 300 s at room temperature. Styrene liquid (Sigma Aldrich, Inc.) was purified by several freeze-pump-thaw cycles before the styrene vapor was admitted into the UHV chamber using a leak valve. Figure 2(a) shows a STM image of a styrene-modified Si (001) surface acquired with tunneling conditions of −2.2 V and 200 pA.

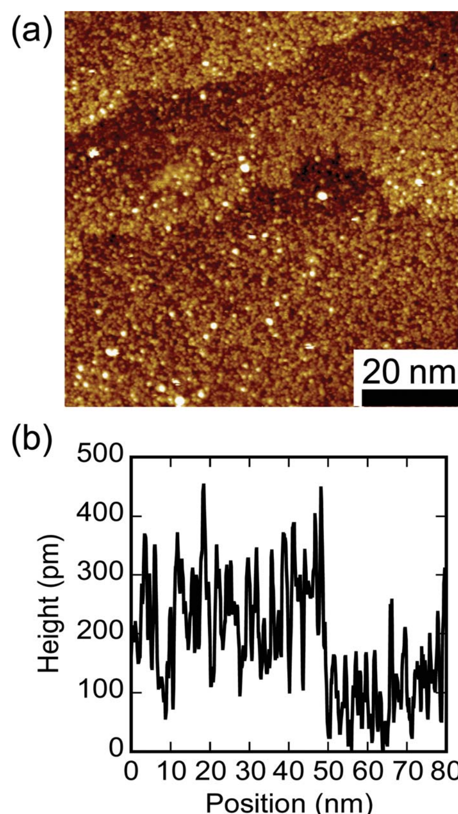

FIG. 2. (Color online) (a) STM image of the styrene-modified Si (001) surface. (b) Height cross section along a line near the top edge of the image, including a single-height Si step.

Under these deposition conditions, styrene does not produce recognizable long-range order at a large coverage of styrene. STM studies with low styrene coverage have reported that a small fraction (~10%) of styrene molecules are found between dimer rows, rather than in the site on top of dimers.[20] At high styrene coverage, the coexistence of the two absorption sites may be sufficient to disrupt the long-range ordering of styrene on the surface. Other molecules, including cyclopentene, form a more highly ordered covalently bonded monolayer on Si (001), but also leave a significant fraction of the surface dimers unreacted even after long exposures to the molecular vapor.[19] Despite the lack of long-range order, the addition of styrene to Si (001) produces a surface in which Si atomic steps can be resolved in STM images as in Figs. 2(a) and 2(b). The roughness of the styrene/Si (001) surface was estimated by averaging the root-mean-square displacement along a large number of 25-nm-long sections of a STM image of a region away from atomic steps. The rms roughness obtained in this way was 73 pm.

Pentacene was deposited onto the styrene-terminated

Author complimentary copy. Redistribution subject to AIP license or copyright, see http://jap.aip.org/jap/copyright.jsp

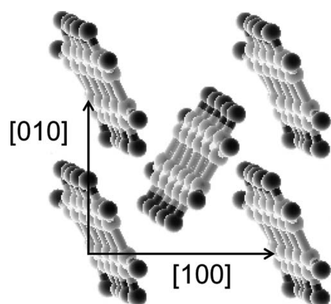

FIG. 3. Molecular model of the (001) surface of a pentacene crystal, based on crystallographic data from Ref. 24.

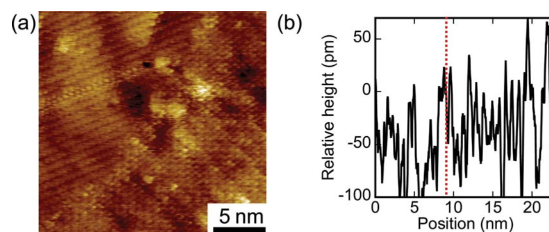

FIG. 5. (Color online) (a) STM image of a tilt grain boundary at the junction between two pentacene islands. (b) Height as a function of position along a line across the grain boundary. The dashed line indicates the location of the grain boundary.

surface from an effusion cell resistively heated to 250 °C. The effective deposition rate was 0.1–0.2 molecular layers/min. The substrate was kept at room temperature for the pentacene growth. The resulting pentacene thin films were imaged using STM with a tunneling current of 300 pA and a bias voltage of −3 V. The same tunneling conditions can be used for imaging pentacene thin films with thicknesses ranging from less than one to seven molecular layers. Each island in the pentacene thin films exhibits a series of terraces exposing (001) or $(00\bar{1})$ crystallographic planes.[23] A schematic of the arrangement of pentacene molecules at the (001) surface of pentacene, based on the bulk structure, is shown in Fig. 3.[24] The two molecules in the crystallographic unit cell extend to different heights with respect to the (001) plane, allowing the in-plane orientation of the pentacene lattice to be identified in STM images.[23]

Islands in the first molecular layer of pentacene completely cover the styrene-modified Si (001) surface. These islands are overgrown by larger second-layer pentacene islands. Each molecular layer after the first layer is faceted, exposing (110) and $(1\bar{1}0)$ edges, as shown in the large-scale STM image encompassing parts of three islands in Fig. 4(a). These are the orientations in which steps are predicted to form with the lowest free energy per unit length.[25]

III. RESULTS AND DISCUSSION

A. Tilt grain boundaries between islands

The first-layer islands in pentacene thin films on styrene-modified Si (001) nucleate independently and do not exhibit a preferred in-plane crystallographic orientation. Tilt grain boundaries form at the junctions between islands, at which the crystallographic orientations of the lattices within the grains are related by a rotation around an axis of rotation normal to {001} planes.[26] The uniform distribution of grain orientations produced by nucleation suggests that the relative orientations of grain boundaries will also be uniformly distributed through all possible misorientation angles. Consistent with this expectation, Kalihari *et al.*[27] showed that 90% of grain boundaries within the first layer of a pentacene thin film on SiO_2 have misorientation angles greater than 15°. The relationship between the crystallographic axes of two contacting islands is shown schematically in Fig. 4(b).

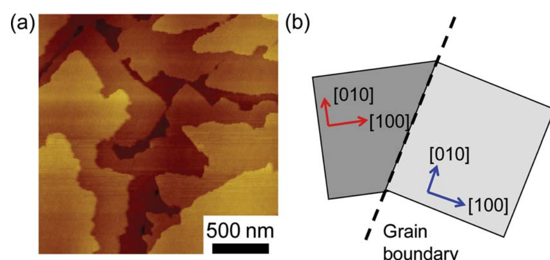

FIG. 4. (Color online) (a) STM image of a pentacene thin film on styrene-modified Si (001). (b) Schematic of the tilt grain boundary between two islands.

An STM image of a tilt grain boundary at the junction between the two islands in the lower half of Fig. 4(a) is shown in Fig. 5(a). The difference in the crystallographic orientations of the two islands is apparent by examining the directions of the rows of molecules in each grain. A cross section of the STM image [Fig. 5(b)] shows that the grain boundary occurs between layers at the same height with respect to the substrate. The misorientation between the two islands in Fig. 5(a) is $67 \pm 2°$.

The grain boundary in Fig. 5(a) does not adopt a uniform crystallographic facet, suggesting that pentacene grain boundaries are kinetically trapped in a state in which a variety of orientations are present. Several segments of the grain boundary in Fig. 5(a) are planar facets with a (110)-type planar orientation with respect to the island occupying the left side of the image. The electronic states resulting from grain boundaries formed on (110) planes have been calculated and predicted to function as charge traps.[28]

B. Grain boundaries between pentacene molecular layers

A second distinct type of grain boundary occurs between the molecular sheets of the pentacene thin films. These twist grain boundaries are located along the {001} planes, separating layers related by a rotation around an axis of rotation normal to {001} planes. A rotation of molecular layer to form a grain boundary along {001} planes is structurally favorable in part because the {001} planes have the lowest surface energy of all pentacene facets.[25]

The in-plane orientation of the pentacene crystal lattice within individual layers of the pentacene film was determined using a series of STM images of each molecular layer. An image showing parts of the second and the third molecular layers of one island in a pentacene thin film are shown in Fig. 6(a). The cross section in Fig. 6(b) shows that the heights of two layers differ by one pentacene layer thickness.

Author complimentary copy. Redistribution subject to AIP license or copyright, see http://jap.aip.org/jap/copyright.jsp

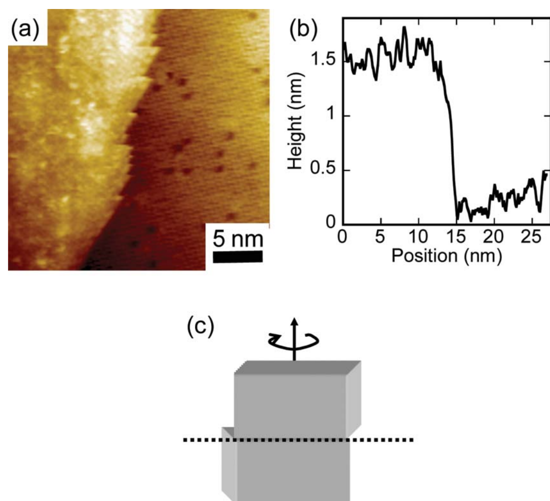

FIG. 6. (Color online) (a) STM image of the second and the third molecular layers of one island in a pentacene thin film on styrene/Si (001). A twist grain boundary is located between these layers. (b) Cross section illustrating the height difference between the two layers. (c) Illustration of the twist grain boundary formed between the layers.

The in-plane orientations of the pentacene lattice within the two layers differ by a rotation of $57 \pm 2°$ around the surface normal, Fig. 6(c). A separate series of images of molecular layers formed on top of the third layer in the same island shows that the crystallographic orientation of the pentacene is the same in the third, the fourth, and the fifth molecular layers.

One potential origin of the twist boundaries between molecular layers lies in the difference in the size of pentacene grains in different layers of the pentacene thin film. The lateral overgrowth of large islands over small islands can produce twist boundaries purely as a result of the island geometry, as shown schematically in Fig. 7(a). An example of this effect is shown in the AFM image of a pentacene thin film grown on the SiO_2 in Fig. 7(b). A pentacene thin film with a

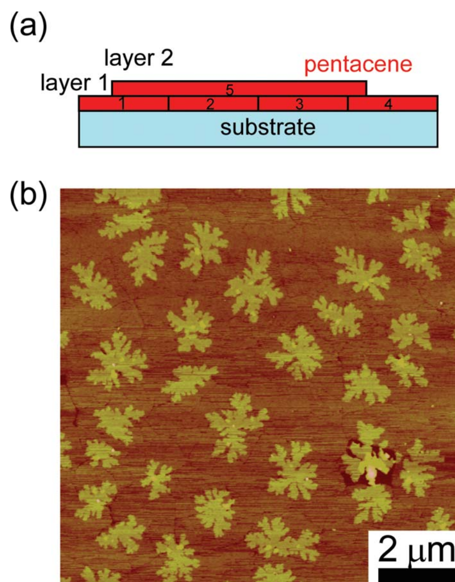

FIG. 7. (Color online) (a) Schematic of a large second-layer island of pentacene (5) grown across several smaller first-layer islands (1–4). (b) AFM image of a 1.2 ML pentacene thin film on SiO_2.

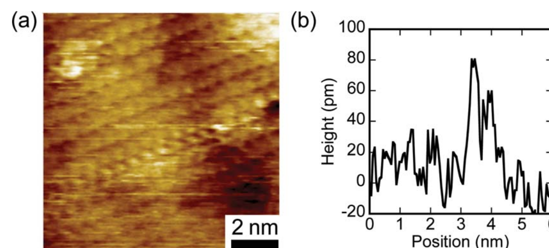

FIG. 8. (Color online) (a) Enlarged STM image of the stacking fault appearing in Fig. 5(a). (b) Cross section showing the height difference of 60 pm between molecules at the stacking fault and molecules in the remainder of the pentacene island.

total thickness of 1.2 molecular layers was deposited onto an oxidized Si substrate held at room temperature in a background pressure of 10^{-6} Torr at a deposition rate of 0.17 layers/min. Islands in the first and second molecular layers are visible in Fig. 7(b). Several of the smaller 100 nm scale first-layer islands are bridged by far larger second-layer islands that have lateral sizes on the order of 1 μm or more. The second-layer islands grow across the grain boundaries between the first-layer islands and produce a series of new grain boundaries between molecular layers parallel to the {001} planes. The twist boundaries created in this way have a completely random distribution of misorientation angles.

A second potential mechanism for the formation of interlayer twist boundaries arises from the independent nucleation of each subsequent layer of molecules. The multilayer island structures of the pentacene thin film result from the nucleation of higher layers when the supersaturation of deposited molecules is sufficient to nucleate a new island. The nucleation results from a thermal fluctuation and is inherently random in other epitaxial systems.[29] The nucleation process can result in structural configurations in which the molecular structure reaches a local minimum of free energy that is different from the bulk crystal structure. Local minima associated with specific twist boundary orientations are structurally similar to those associated with organic epitaxy and quasiepitaxy, particularly in systems in which there is a close match of lattice parameters.[1,30] Using the thin-film lattice constants given by Mannsfeld *et al.*,[31] the EPICALC software package[32] predicts that there are several potentially favorable arrangements of a rotated pentacene overgrowing an underlying pentacene layer. A rotation of 76° between layers, for example, allows half of the molecules in the upper pentacene layer to occupy sites with a spacing appropriate for a continuation of the crystal.[33] The 57° rotation across the twist boundary in Fig. 6(a) is not among the angles predicted to have a low free energy. We therefore conclude that this particular grain boundary resulted from overgrowth rather than from nucleation.

C. Stacking faults

Extended structural defects are also found within individual islands. The image of the grain boundary in Fig. 5(a) includes a stacking fault, an interruption in the repeating pattern of high and low molecules. Figure 8(a) shows an enlarged image of the vicinity of the stacking fault. The stacking fault in Fig. 8(a) is clearly strongly faceted, occupying a

Author complimentary copy. Redistribution subject to AIP license or copyright, see http://jap.aip.org/jap/copyright.jsp

single (100) plane in which a row of molecules is missing. Each of the molecules in the missing row occupies the apparently low molecular basis site in STM images. Stacking faults observed in other organic molecular materials also appear to be confined to a single molecular plane.[8]

One row on each side of the geometric plane of the stacking fault appears higher in the STM images than the molecules far from the stacking fault. The height difference is apparent in the plot of the height as a function of position along a line across the stacking fault in Fig. 8(b), in which the molecules near the fault have an apparent height of 60 pm higher than the neighboring molecules. The height plotted in Fig. 8(b) is an average over a 1-nm-wide section of the image. A difference in height has been reported across large distances in previous STM studies and shown in calculations to lead to large variations in the energy levels of both holes and electrons for height differences as small as 50 pm.[18] Similarly large variations in electronic structure result from in-plane shifts in the molecular positions similar to those found at the stacking fault.[34] Stacking faults may thus be important contributors of defect-related electronic states in pentacene thin film.

IV. CONCLUSION

Pentacene thin films encompass a range of extended defects other than those reported in the literature within pentacene thin films grown on modified Si (001) surfaces. Imaging and understanding these types of defects structurally allow their energies and electronic properties to be calculated. Using this knowledge, the effect of extended defects on electronic transport can be understood. The resulting ideas will lead to understanding and controlling defects in organic-organic or in organic-inorganic interfaces.

Transport studies describing the roles of structural defects in degrading the electrical properties of thin-film FETs have often taken a large-scale statistical approach. Studies have shown that dislocations and grain boundaries have important effects on the electrical characteristics of organic thin films.[35,36] Recent experimental developments have permitted the study of individual grains or individual grain boundaries. At a more microscopic scale, high angle grain boundaries cause a decrease in the magnitude of photocurrent in bicrystals.[37] Similarly, using conducting probe AFM, Kelley *et al.*[38] found that the electrical resistance significantly increased across a single grain boundary in sexithiophene crystals. The molecular structure of these defects, however, was not determined in the microscopic studies.

Future advances in fabrication and electrical characterization will allow the electrical properties of grain boundaries with well-defined structures to be determined. Already the effects of the variation in the electronic properties of grain boundaries with their molecular-scale structure is accounted for in some transport models.[39] The high-resolution description of structural defects in the present study can be used to provide insight into other defects in similar structures that are relevant to organic electronic devices.

ACKNOWLEDGMENTS

This work was supported by the Petroleum Research Fund of the American Chemical Society and the University of Wisconsin Materials Research Science and Engineering (NSF Grant No. DMR-0520527). We are grateful to B. N. Park for providing the pentacene/SiO_2 sample.

[1] S. R. Forrest, Chem. Rev. (Washington, D.C.) **97**, 1793 (1997).
[2] C. D. Dimitrakopoulos, I. Kymissis, S. Purushothaman, D. A. Neumayer, P. R. Duncombe, and R. B. Laibowitz, Adv. Mater. (Weinheim, Ger.) **11**, 1372 (1999).
[3] E. Menard, V. Podzorov, S. H. Hur, A. Gaur, M. E. Gershenson, and J. A. Rogers, Adv. Mater. (Weinheim, Ger.) **16**, 2097 (2004).
[4] G. Z. Wang, Y. Luo, and P. H. Beton, Appl. Phys. Lett. **83**, 3108 (2003).
[5] A. B. Chwang and C. D. Frisbie, J. Appl. Phys. **90**, 1342 (2001).
[6] B. D. Chapman, A. Checco, R. Pindak, T. Slegrist, and C. Kloc, J. Cryst. Growth **290**, 479 (2006).
[7] M. Eremtchenko, R. Temirov, D. Bauer, J. A. Schaefer, and F. S. Tautz, Phys. Rev. B **72**, 115430 (2005).
[8] T. Maeda, T. Kobayashi, T. Nemoto, and S. Isoda, Philos. Mag. **81**, 1659 (2001).
[9] P. K. Miska, L. F. Drummy, and D. C. Martin, Mater. Res. Soc. Symp. Proc. **734**, A5.4.1 (2003).
[10] B. Nickel, R. Barabash, R. Ruiz, N. Koch, A. Kahn, L. C. Feldman, R. F. Haglund, and G. Scoles, Phys. Rev. B **70**, 125401 (2004).
[11] J. S. Wu and J. C. H. Spence, J. Appl. Crystallogr. **37**, 78 (2004).
[12] L. F. Drummy, C. Kubel, D. Lee, A. White, and D. C. Martin, Adv. Mater. (Weinheim, Ger.) **14**, 54 (2002).
[13] T. Ando, A. B. Fowler, and F. Stern, Rev. Mod. Phys. **54**, 437 (1982).
[14] B. N. Park, S. Seo, and P. G. Evans, J. Phys. D: Appl. Phys. **40**, 3506 (2007).
[15] R. Ruiz, B. Nickel, N. Koch, L. C. Feldman, R. F. Haglund, A. Kahn, and G. Scoles, Phys. Rev. B **67**, 125406 (2003).
[16] F.-J. Meyer zu Heringdorf, M. C. Reuter, and M. C. Tromp, Nature (London) **412**, 517 (2001).
[17] K. P. Weidkamp, R. M. Tromp, and R. J. Hamers, J. Phys. Chem. C **111**, 16489 (2007).
[18] J. H. Kang, D. da Silva Filho, J.-L. Bredas, and X.-Y. Zhu, Appl. Phys. Lett. **86**, 152115 (2005).
[19] R. J. Hamers, S. K. Coulter, M. D. Ellison, J. S. Hovis, D. F. Padowitz, C. M. Greenlief, and J. N. Russell, Acc. Chem. Res. **33**, 617 (2000).
[20] M. P. Schwartz, M. D. Ellison, S. K. Coulter, J. S. Hovis, and R. J. Hamers, J. Am. Chem. Soc. **122**, 8529 (2000).
[21] A. Calzolari, A. Ruini, E. Molinari, and M. J. Caldas, Phys. Rev. B **73**, 125420 (2006).
[22] M. Meuris, P. W. Mertens, A. Opdebeeck, H. F. Schmidt, M. Depas, G. Vereecke, M. M. Heyns, and A. Philipossian, Solid State Technol. **38**, 109 (1995).
[23] S. Seo, L. C. Grabow, M. Mavrikakis, R. J. Hamers, N. J. Thompson, and P. G. Evans, Appl. Phys. Lett. **92**, 153313 (2008).
[24] R. B. Campbell, J. M. Robertson, and J. Trotter, Acta Crystallogr. **14**, 705 (1961).
[25] J. E. Northrup, M. L. Tiago, and S. G. Louie, Phys. Rev. B **66**, 121404 (2002).
[26] P. E. J. Flewitt and R. K. Wild, *Grain Boundaries: Their Microstructure and Chemistry* (Wiley, New York, 2001).
[27] V. Kalihari, E. B. Tadmor, G. Haugstad, and C. D. Frisbie, Adv. Mater. (Weinheim, Ger.) **20**, 4033 (2008).
[28] S. Verlaak and P. Heremans, Phys. Rev. B **75**, 115127 (2007).
[29] W. Theis and R. M. Tromp, Phys. Rev. Lett. **76**, 2770 (1996).
[30] S. C. B. Mannsfeld and T. Fritz, Mod. Phys. Lett. B **20**, 585 (2006).
[31] S. C. B. Mannsfeld, A. Virkar, C. Reese, M. F. Toney, and Z. N. Bao, Adv. Mater. (Weinheim, Ger.) **21**, 2294 (2009).
[32] D. E. Hooks, T. Fritz, and M. D. Ward, Adv. Mater. (Weinheim, Ger.) **13**, 227 (2001).
[33] V. Kalihari, D. J. Ellison, G. Haugstad, and C. D. Frisbie, Adv. Mater. (Weinheim, Ger.) **21**, 3092 (2009).
[34] J. L. Bredas, J. P. Calbert, D. A. da Silva, and J. Cornil, Proc. Natl. Acad. Sci. U.S.A. **99**, 5804 (2002).
[35] A. Bolognesi, M. Berliocchi, M. Manenti, A. Di Carlo, P. Lugli, K. Lmi-

Author complimentary copy. Redistribution subject to AIP license or copyright, see http://jap.aip.org/jap/copyright.jsp

mouni, and C. Dufour, IEEE Trans. Electron Devices **51**, 1997 (2004).
[36] Y.-Y. Lin, D. I. Gundlach, S. F. Nelson, and T. N. Jackson, IEEE Trans. Electron Devices **44**, 1325 (1997).
[37] J. Liao and D. C. Martin, Macromolecules **29**, 568 (1996).
[38] T. W. Kelley, E. L. Granstrom, and C. D. Frisbie, Adv. Mater. (Weinheim, Ger.) **11**, 261 (1999).
[39] R. A. Street, J. E. Northrup, and A. Salleo, Phys. Rev. B **71**, 165202 (2005).

Author complimentary copy. Redistribution subject to AIP license or copyright, see http://jap.aip.org/jap/copyright.jsp